

Defect Detection in Large CT Image Sets



Douglas N. Poland
(925) 422-4980
poland1@llnl.gov

This image analysis project has constructed a tool for performing computer-assisted detection of small voids in CT data sets of metal components. We first constructed algorithms using known approaches and measured their performance on a test object, described below. Noise reduction and void detection algorithms based on mathematical morphology demonstrated good performance on the test object and excellent performance on a small but diverse collection of programmatic data sets that had been previously analyzed manually. Implementation issues, such as handling large data sets and automated parameter selection, have been explicitly addressed in the course of working with these data. The result is a standalone C++ application, delivered to the enhanced surveillance program that directs a tomography analyst's attention to candidate void regions in large data sets.

Project Goals

The enhanced surveillance program will produce CT data sets that are up to several thousand voxels on a side (*i.e.*, 8000 x 8000 x 8000). The current method of analysis requires a tomographer to view sequences of several thousand images, where each image occupies several computer screens at full resolution. One of the primary objectives is to identify voids of any size. The work of searching for voids at the resolution limit of the system is extremely demanding and tedious in these data sets. The goal of this project is to create a tool that will reduce these data sets to a ranked set of candidate voids that can be quickly validated or rejected by the tomographer; the broader goal is to strengthen the dialog and technical exchange between tomography and image analysis experts so that emerging image analysis issues can be effectively addressed.

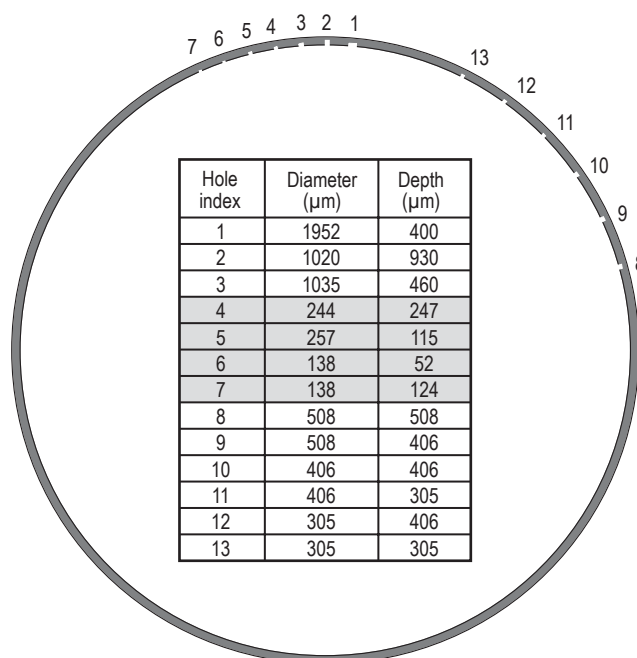
The enhanced surveillance program uses a tungsten ring with holes drilled into it (Fig. 1) to study the ability of their systems and analysts to detect small voids

in metal parts. Of the 13 holes in this ring, 9 (ranging from 305 to over 1000 mm in diameter) are well resolved by the CT system and are readily discernible in the processed CT data (the remaining 4 are less than 300 mm in diameter). One key success metric is that our algorithm must place these 9 voids at the top of our ranked list of candidate voids.

Relevance to LLNL Mission

This project has produced a tool that will increase the efficiency of enhanced surveillance program tomography analysts by focusing their attention on suspect voids in a given data set, thereby allowing them to forego an exhaustive search of many thousands of screens of largely defect-free data. This tool could also make these data sets more accessible to other technical staff, who may not be tomography experts, by performing necessary preprocessing and quickly guiding them to regions with suspect voids. This application should be generally applicable to the detection of small defects (*i.e.*, voids and inclusions) in homogeneous media.

Figure 1. Tungsten ring test object, a cylinder with 13 holes drilled into its inner surface. This cutaway sketch shows the hole locations, while the table lists their sizes. Note that in the images used for this work, holes #4 through #7 are very difficult to impossible to detect manually. They are not found by our algorithms.



FY2007 Accomplishments and Results

We accomplished four interrelated tasks in FY2007: 1) algorithm testing and refinement using programmatic data sets; 2) automated parameter selection; 3) implementation in C++; and 4) identification of issues that warrant future work. We have delivered a standalone C++ application that effectively focuses an analyst's attention on localized anomalies in large grayscale 3-D CT data sets.

In the course of testing with these data sets, we have refined the way that we calculate ranking metrics for candidate voids, using, for example, a contrast calculation that handles region boundaries (Fig. 2). Our revised volume-weighted contrast ranking performs well on the tungsten ring defects (9 detected

holes ranked in order of decreasing size, with the most conspicuous false alarm ranked number 10 (Fig. 3)).

We have implemented a minimum entropy approach to calculating the void detection threshold parameter, and also a second threshold to yield a more complete void reconstruction (Fig. 4). We have also achieved a 4x speedup, as well as portability and improved data and memory management, with our optimized C++ implementation leveraging published methods.

Related References

1. Haralick, R., S. Sternberg, and X. Zhuang, "Image Analysis Using Mathematical Morphology," *IEEE Transactions on Pattern Analysis and Machine Intelligence*, **9**, pp. 532-550, 1987.
2. Rosenberg, A., and J. Hirschberg, "V-Measure: A Conditional Entropy-based Cluster Evaluation Measure," *Proceedings of the 2007 Joint Conference of Empirical Methods in Natural Language Processing and Computational Natural Language Learning*, Prague, pp. 410-420, June 2007.
3. van Herk, M., "A Fast Algorithm for Local Minimum and Maximum Filters on Rectangular and Octagonal Kernels," *Patt. Rec. Letters*, **13**, pp. 517-521, 1992.
4. Bloomberg, D., "Implementation Efficiency of Binary Morphology," *International Symp. for Math. Morphology VI*, Sydney, Australia, April 3-5, 2002.
5. van den Boomgard, R., and R. van Balen, "Methods for Fast Morphological Image Transforms Using Bitmapped Images," *Computer Vision, Graphics, and Image Processing: Graphical Models and Image Processing*, **54**, pp. 254-258, May 1992.

FY2008 Proposed Work

We have identified ideas for future work that may lead to enhanced detection sensitivity and false alarm rejection by performing more sophisticated true and false positive characterization (*e.g.*, classification techniques operating on shape, density, texture, and other features in both the candidate defect and surrounding background regions).

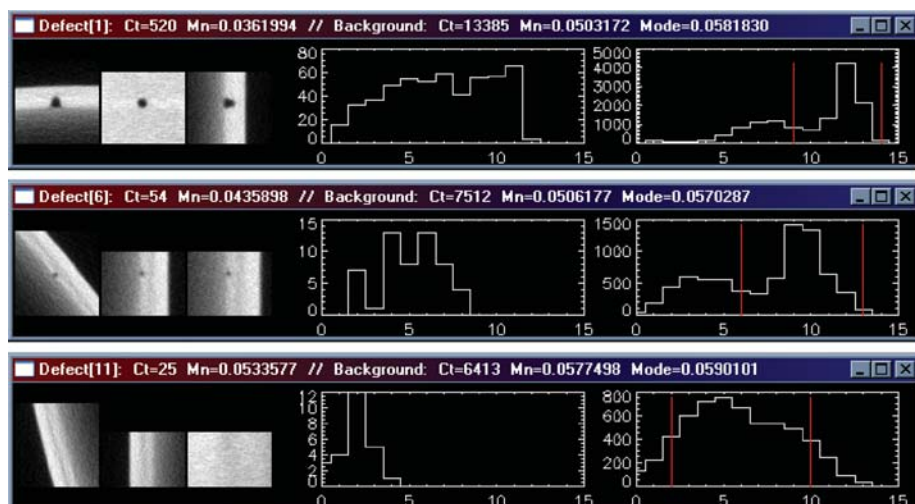


Figure 2. Three candidate defects ranked 1, 6 and 11 by the detection code. For each defect we display (from left to right): x-y, x-z and y-z views; defect voxel intensity histogram; and immediate background voxel intensity histogram. Defects 1 and 6 are true positives, (corresponding to holes #2 and #11 from Fig. 1, respectively) that occur on a region boundary. Their background histograms are bi-modal, with the relevant background intensity captured by the primary mode (defined by the vertical red lines that are generated automatically). Using this primary mode in the contrast calculation improves the ranking metric. The size of the W ring CT data set is 1908 x 1908 x 56. The thumbnails shown are all 64 voxels on a side, displayed at full resolution.

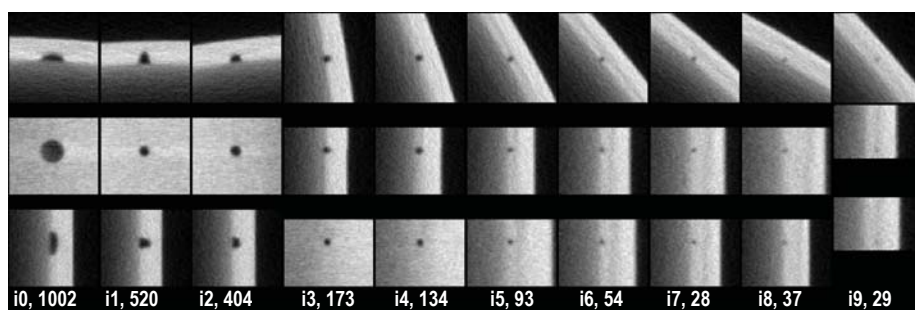


Figure 3. The top 10 ranked tungsten ring candidate defects (in 10 columns above) produced by our application. Rank proceeds from left to right, with x-y, x-z and y-z views (top to bottom) shown for each candidate.

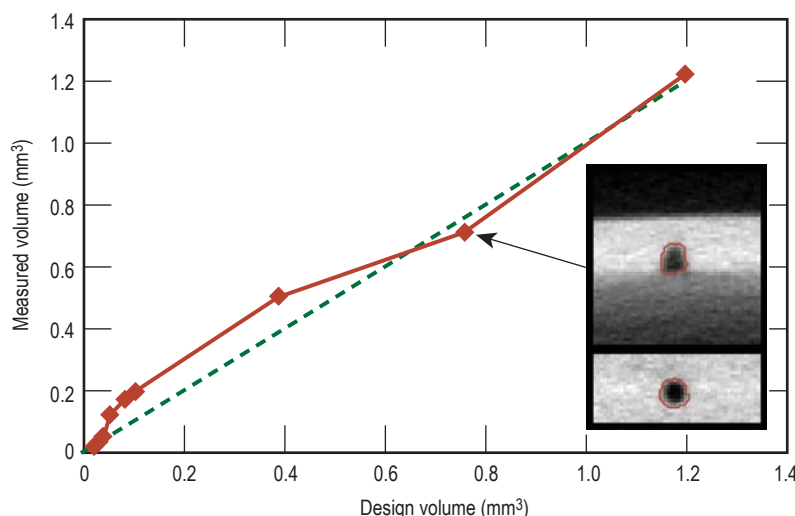


Figure 4. Plot of measured tungsten (brown line) defect volumes vs. design (green dashed line) volumes. Measured volumes were calculated using "double-threshold" morphological reconstruction.